

Electrochemical performance of a new imidazolium ionic liquid crystal and carbon paste composite electrode for the sensitive detection of paracetamol

R. Mangaiyarkarasi^a, S. Premlatha^b, Rajkumar Khan^c, R. Pratibha^c, S. Umadevi^{a,*}

^a Department of Industrial Chemistry, School of Chemical Sciences, Alagappa University, Karaikudi 630003, India

^b School of Material Science and Engineering, School of Chemistry and Chemical Engineering, Jiangsu University, Zhenjiang 212013, PR China

^c Raman Research Institute, C. V. Raman Avenue, Sadashivanagar, Bangalore 560 080, India

ARTICLE INFO

Article history:

Received 19 April 2020

Received in revised form 4 September 2020

Accepted 6 September 2020

Available online 11 September 2020

Keywords:

Biphenyl core

Ionic liquid crystal

Smectic A

Composite electrode

Paracetamol sensing

ABSTRACT

A new ionic liquid crystal (ILC) bearing a biphenyl core and a terminal imidazolium moiety was synthesized which exhibited two enantiotropic smectic A mesophases having a wide phase range. Interestingly one of these mesophases exhibited the features of a biaxial phase. A composite electrode containing the synthesized ILC and carbon paste (CP) was fabricated and employed for the successful electrochemical detection of a clinically important analgesic drug, paracetamol. The ILC-CP composite electrode displayed an enhanced current response due to a versatile combination of properties namely, good ionic conductivity, increased edge-site defects and excellent electrocatalytic activity. The composite electrode responded quickly upon addition of paracetamol and the peak current of anodic oxidation enhanced at lower over potential compared to the carbon paste electrode (CPE). Differential pulse voltammetric (DPV) experiments for the detection of paracetamol yielded acceptable linear range from 0 to 120 μM with a good detection limit of 2.8 μM . Interference test results showed anti-interfering ability in presence of a mixture of interferents. The electrode stability was evaluated from DPV current response and 92.6% current was retained after one month which revealed the excellent stability. The electrode was successfully applied for the direct determination of paracetamol in pharmaceutical formulations.

© 2020 Elsevier B.V. All rights reserved.

1. Introduction

Over the past decades, a myriad of fascinating liquid crystals (LCs) have been synthesized and find applications in various fields [1–5]. Ionic liquid crystals (ILCs) are a section of LCs with blended properties of ionic liquids (ILs) and LCs [6]. ILCs solely consist of ions and form fluid mesophases via numerous non-covalent interactions such as electrostatic and hydrophobic interactions. ILCs display different mesophases similar to their non-ionic thermotropic counterparts namely, nematic, smectic and columnar phases, although smectic A (SmA) phase is the commonly observed mesophase [7,8]. SmA phase has the orthogonal arrangement of molecules, that is, the molecules are arranged in layers and their long molecular axes, on average, are parallel to the layer normal. The molecules can rotate freely along their long axes in SmA phase and therefore the phase is optically uniaxial. If the free rotation of the molecules along their long axes is restricted, the molecules will have an additional lateral order within the layers resulting in a biaxial phase. Such orthogonal biaxial LC phase (SmA_b) was predicted theoretically by de Gennes [9] and has attracted significant attention both from fundamental and application point of view. Generally, the board-like molecules (or

association of the molecules resulting in board-like structure) are expected to show the SmA_b mesophase. This phase has been observed experimentally in some of the thermotropic LC compounds; polymeric systems, mixture of bent and rod-like compounds, metallomesogens, pure bent-core compounds and non symmetric LC dimers [10–13]. However, to the best of our knowledge, so far, there is no report of SmA_b in an ILC system and is yet to be realized.

ILCs exhibit interesting properties such as ease of macroscopic orientation, high ionic conductivity, good electrochemical window and better charge storage and transport [14,15]. Owing to their remarkable properties, ILCs have been intensively investigated as electrolyte and electrode materials for many electrochemical applications such as supercapacitors, batteries, sensing etc. [16–18]. Recently, we also reported the synthesis and characterization of cholesterol containing imidazolium ILC and its dual application as an electrolyte and electrode material [19].

Carbon paste electrodes (CPE) play a crucial role in electroanalysis owing to their unique properties like facile to fabricate, renewability of the electrode surface, low background current, stable response, low cost, versatile modification and simple kinetics involved in electrode processes which are convenient for the detection of organic as well as biological analytes [20–22]. Currently, ILs having high ionic conductivity and inherent electrocatalytic activity have been used along with carbon paste during the preparation of CPEs, since the resulting composite electrode offer

* Corresponding author.

E-mail address: umadevis@alagappauniversity.ac.in (S. Umadevi).

beneficial features such as high sensitivity, lower over potential and anti-fouling properties [23]. For instance, Hadi Beitollahi et al. reported studies on IL and Au NPs modified CPEs for sensing thyroid-stimulating hormone [24]. ILCs have close resemblance to the properties of ILs such as negligible vapour pressure, good thermal stability, wide electrochemical window and also possess interesting properties of LCs namely self-assembling ability, molecular order and anisotropic properties [6,7,25]. ILC modified CPE surface is expected to have a layered morphology, which can induce more edge-plane sites on the electrode surface. A high density of edge-plane-like defects on the surface can increase the kinetics of electrode for many redox reactions, reduce the passivation effects, impart the anti-fouling property and improve the reproducibility, stability and sensitivity of the electrode [26,27]. Owing to these remarkable properties, ILC modified CPEs have been explored for the electrochemical sensing of drugs and neurotransmitters [28,29].

Paracetamol or acetaminophen is a well-known analgesic, antipyretic and anti-inflammatory drug widely administered for the viral/bacterial fevers and mild to moderate pain relief associated with headache, toothaches, arthritis, backaches, and post-operative pains. The pKa value of paracetamol is 9.5 which easily get absorbed by the cells and excreted in the urine [30]. In general, paracetamol intake does not manifest any harmful side effects in therapeutic doses but, the overdose of this drug could lead to inflammation of pancreas, glutathione depletion, fulminating hepatic necrosis, kidney damage and hepatotoxicity [31]. The oral administration of paracetamol in children above one year can cause an increase in asthma, and rhinoconjunctivitis [32]. Therefore, the detection of paracetamol is necessary and has gained extensive attention among the researchers worldwide.

Since paracetamol is electrochemically active, electrochemical detection is emerging as better method due to its key advantages such as cost effectiveness, extreme sensitivity, ease of preparation, and miniaturization possibilities for electroanalysis of paracetamol. However, on conventional electrodes, paracetamol is not easily oxidized and exhibit poor response because of its sluggish electrode kinetics. Hence, chemically modified electrodes were developed in recent years, which were successfully utilized in electrochemical sensor fabrication [33–37]. Recently, carbon paste electrodes modified with ILCs were explored as electrochemical sensors for the determination of drugs and compounds. For instance, Galal, and his co-workers reported studies on piperidinium based ILC modified CPE for electroanalysis of antihypertensive drug [38,39] and described commercial ILCs/Au NPs/carbon nanotubes modified CPE for paracetamol sensing applications [40]. Moreover, the same research group reported cyclodextrin and ILC modified graphene composite electrode for detection of some neurotransmitters [41].

Herein, we reported the synthesis of a new imidazolium based ILC compound, its mesomorphic behaviour and application of this ILC as an electrode material in combination with carbon paste for the detection of paracetamol. The ILC is dimesomorphic and exhibited a high temperature uniaxial SmA and a low temperature biaxial SmA phase with a wider phase range. Composite electrodes were prepared by employing the ILC and carbon paste (30:70 wt%) by heating the ILC to different temperatures (rt, 90 °C, 120 °C) and the electrochemical performance of the resulting ILC-CP composite electrodes was evaluated. The ILC-CPE electrode displayed an improved response compared to the unmodified CPE. Further, the detection of paracetamol using the newly fabricated electrode, studies on stability, sensitivity and selectivity of the electrode for the sensing of paracetamol are presented. Real sample analysis of the paracetamol in pharmaceutical drug formulation was also conducted.

2. Experimental

2.1. Materials

11-Bromoundecanoic acid, 4-(dimethylamino) pyridine (DMAP), *N,N'*-diisopropyl carbodiimide (DIC), acetaminophen (PA), nitrophenol

(NP), dopamine (DA), buffer tablets (pH = 7) and 1-methyl imidazole were obtained from Sigma Aldrich. Glucose (Glu), uric acid (UA), ascorbic acid (AA) and potassium chloride (KCl) were bought from TCI chemicals. All the chemicals were used as purchased, except 1-methylimidazole, which was distilled prior to conduct the reaction. The solvents were purified and dried using conventional methods.

2.2. Methods

Chemical structure of the synthesized compounds was characterized using infrared (IR), nuclear magnetic resonance (NMR) spectroscopy and mass spectrometry techniques. IR spectra were recorded on a Bruker Tensor 27 FTIR spectrometer (Bruker Optic GmbH, Germany) using KBr pellets. ¹H NMR spectra were recorded on a Bruker Avance 400 MHz spectrometer (Bruker, Switzerland) using tetramethylsilane as an internal standard. Liquid crystalline behaviour of ILC, **A** was examined using a combination of differential scanning calorimetry (DSC), polarizing optical microscopy (POM) and X-ray diffraction studies (XRD). Phase transition temperatures were obtained from thermograms recorded on a Perkin Elmer DSC (DSC 6000, Perkin Elmer, US) with a heating and cooling rate of 10 °C/min. Textural observations were carried out using a Olympus BX50 POM (Olympus Co., Japan) equipped with a Linkam LTS 420E (Linkam, UK) heating stage having a T95-HS Link controller. The X-ray diffraction patterns of the sample were collected from PANalytical, (Model-Empyrean, Netherlands) X-ray diffractometer by employing Cu-K_α (λ = 1.54 Å) radiation. Molecular mass of ILC was determined using a JEOL GCMATE II GC-MS, USA. Moreover, Scanning electron microscope (SEM) observations were carried out using FEI Quanta 250 (FEI Corporation, Japan) instrument. ILC dissolved in chloroform was drop-casted on indium tin oxide (ITO) plate, dried at room temperature and viewed under the SEM. Electrochemical studies were performed using an AutolabPGSTAT30 Potentiostat/Galvanostat electrochemical workstation (EcoChemi, Netherlands) with a three electrode system consisting of Ag/AgCl as a reference electrode, platinum wire as a counter electrode and ILC modified CP as a working electrode. A PBS buffer solution having pH = 7.0 was used as an electrolyte for sensor studies.

For the interference studies, differential pulse voltammetry (DPV) experiments were conducted in phosphate buffer solution (PBS) at a scan rate of 50 mVs⁻¹. Initially, 50 μM of paracetamol solution was added to PBS (pH = 7) and the corresponding DPV curve was recorded. Soon after, 5-fold increased concentration of other possible interferents such as dopamine, ascorbic acid, KCl, nitrophenol, uric acid, glucose were added one by one to the same electrolyte and their corresponding DPV current response was recorded.

2.3. Synthesis of 4'-(decyloxy)-[1,1'-biphenyl]-4-ol, **b**

4,4'-Dihydroxy biphenyl (3 g; 16.1 mmol) was dissolved in dry ethanol (30 mL), sodium hydroxide (0.644 g; 16.1 mmol) was added to the reaction mixture and then refluxed until colour of the solution was changed to dark green. Subsequently, 1-bromodecane (3.4 mL; 16.1 mmol) was added and continuously refluxed for 3 h at 80 °C. After that, the reaction mixture was cooled to room temperature. The reaction mixture was acidified with 5 mL of con. HCl to get a precipitate which was then washed with ethanol and dried under vacuum. The residue was dissolved in ethanol: acetic acid (1:1) and then undissolved impurities were removed by filtration. Further, the product was purified by column chromatography on silica gel using dichloromethane (CH₂Cl₂) and ethyl acetate as an eluent (9:1) to get compound **b** as a white powder. Yield: 40%

FTIR (KBr) ν_{max} : 3304, 2944, 2855, 1874, 1610, 1498, 1455, 1386, 1252, 1127, 1036, 803, 725, 648, 561, 510 cm⁻¹.

¹H NMR (400 MHz, CDCl₃) δ (ppm): 9.82 (s, OH, 1H), 7.51 (d, Ar-H, 2H, ³J = 8.4 Hz), 7.45 (d, Ar-H, 2H, ³J = 8.4 Hz), 6.97 (d, Ar-H, 2H, ³J = 8.4 Hz), 6.91 (d, Ar-H, 2H, ³J = 8.4 Hz), 4.05 (t, -O-CH₂, 2H, ³J = 6.8 Hz),

1.92–1.83 (m, $-\underline{\text{CH}}_2$, 2H), 1.56–1.4 (m, $-\underline{\text{CH}}_2$, 14H), 0.94 (t, $-\underline{\text{CH}}_3$, 3H, $^3J = 6.4$ Hz).

2.4. Synthesis of 4'-(decyloxy)-[1,1'-biphenyl]-4-yl 11-bromoundecanoate, **c**

Compound **b**, 4'-(decyloxy)-[1,1'-biphenyl]-4-ol (2 g; 6 mmol) was dissolved in dry chloroform (20 mL), 11-bromoundecanoic acid (1.6 g; 6 mmol), DMAP (0.0073 g; 0.06 mmol) were added to the solution and the resulting mixture was stirred for 30 min. Afterwards, DIC (1.043 mL; 6.73 mmol) was added and continuously stirred for 24 h at ambient condition. Thereafter, excess solvent present in the reaction mixture was evaporated in vacuum. The residue obtained was purified by column chromatography on silica gel using hexane and ethyl acetate as an eluent (9:1) to afford compound **c**. The product was further purified through recrystallization from acetonitrile. Yield: 65%

FTIR (KBr) ν_{max} : 3444, 2919, 1746, 1610, 1495, 1384, 1227, 1150, 1031, 820, 724, 506 cm^{-1} .

$^1\text{H NMR}$ (400 MHz, CDCl_3) δ (ppm): $^1\text{H NMR}$ (400 MHz, CDCl_3) δ (ppm): 7.52 (d, Ar-H, 2H, $^3J = 8.4$ Hz), 7.43 (d, Ar-H, 2H, $^3J = 8.4$ Hz), 7.11 (d, Ar-H, 2H, $^3J = 8.4$ Hz), 6.95 (d, Ar-H, 2H, $^3J = 8.4$ Hz), 4.10 (t, $-\text{O}-\underline{\text{CH}}_2$, 2H, $^3J = 6.8$ Hz), 3.42 (t, $-\underline{\text{CH}}_2$ -Br, 2H, $^3J = 6.8$ Hz), 2.63 (t, $-\underline{\text{CH}}_2$, 2H, $^3J = 7.6$ Hz), 2.01–1.52 (m, $-\underline{\text{CH}}_2$, 2H), 1.54–1.35 (m, $-\underline{\text{CH}}_2$, 30 H), 0.94 (t, $-\underline{\text{CH}}_3$, 3H, $^3J = 6.4$ Hz).

2.5. Synthesis of 4'-(decyloxy)-[1, 1'-biphenyl]-4-yl 11-(3-methylimidazolidin-yl) undecanoate, bromide salt, **A**

A solution of compound **c** (0.5 g; 8.7 mmol) and 1-methylimidazole (0.143 mL; 1.7 mmol) in dry toluene (5 mL) was stirred vigorously in a pressure tube at 90 °C for 120 h, under nitrogen atmosphere. Thereafter, excess solvent from the reaction mixture was evaporated in vacuum. The white precipitate obtained was washed twice using diethyl ether in order to remove the unreacted starting material. The product obtained after washing was further purified by flash-column chromatography on silica gel (eluant: CH_2Cl_2 -methanol in the ratio 9:1) to give the pure product **A** as a white powder. Yield: 68%

FTIR (KBr) ν_{max} : 3429, 3092, 2925, 2861, 1746, 1593, 1496, 1225, 1150, 1041, 818, 612, 523 cm^{-1} .

$^1\text{H NMR}$ (400 MHz, CDCl_3) δ (ppm): 10.39 (s, N-CH-N, 1H), 7.56 (d, Ar-H, 2H, $^3J = 8.4$ Hz), 7.49 (d, Ar-H, 2H, $^3J = 8.4$ Hz), 7.35 (s, Imi-H, 2H), 7.13 (d, Ar-H, 2H, $^3J = 8.4$ Hz), 6.97 (d, Ar-H, 2H, $^3J = 8.4$ Hz), 4.34 (t, $-\text{OCH}_2$, 2H, $^3J = 7.2$ Hz), 4.12 (s, N-CH₃, 3H), 4.01 (t, Imi-CH₂-CH₂-, 2H, $^3J = 6.8$ Hz), 2.61 (t, $-\underline{\text{CH}}_2$, 2H, $^3J = 7.6$ Hz), 1.9–1.7 (m, $-\underline{\text{CH}}_2$, 2H), 1.4–1.3 (m, $-\underline{\text{CH}}_2$, 30H), 0.91 (t, $-\underline{\text{CH}}_3$, 3H, $^3J = 6.4$ Hz). $^{13}\text{C NMR}$ (500 MHz, CDCl_3) δ (ppm) 172.7, 159.0, 149.8, 138.7, 138.2, 132.8, 128.2, 127.8, 123.3, 121.9, 121.7, 115.0, 68.3, 50.5, 37.0, 34.5, 32.0, 31.1, 30.4, 29.7, 29.5, 29.3, 29.2, 29.1, 29.0, 26.3, 26.2, 25.0, 22.8, 14.2. HRMS (SI): m/z calcd for $[\text{C}_{37}\text{H}_{55}\text{BrN}_2\text{O}_3]^+$: 655.756, found: 655.7520 $[\text{M}-\text{Br}]^+$. Elemental analysis for $\text{C}_{37}\text{H}_{55}\text{BrN}_2\text{O}_3$: Calculated-C:67.7%; H: 8.39%; N: 4.27%; Found C: 67.57%; H: 8.40%; N: 4.27%

IR spectra for compounds **b**, **c** and **A** are provided in Fig. S1. $^1\text{H NMR}$ spectra along with assignment of the signals for compounds **c** and **A** are provided in Figs. S2 and S3. $^{13}\text{C NMR}$ spectrum for compound **A** is given in Fig. S4 and mass spectrum for **A** is given in Fig. S5 of the electronic Supplementary information (SI).

2.6. Fabrication of the electrode

Old pen refills were collected and cut into an appropriate length of 4 cm long. After that the refill tubes were sonicated in ethanol and acetone for 30 min in order to remove impurities. ILC modified CPE was prepared by mixing graphite: ILC in the ratio 70:30, along with few drops of paraffin oil. The resultant homogeneous paste was tightly packed into the cavity of refill tubes. The electrical contact was established through a brass wire. The fabricated electrode surface was

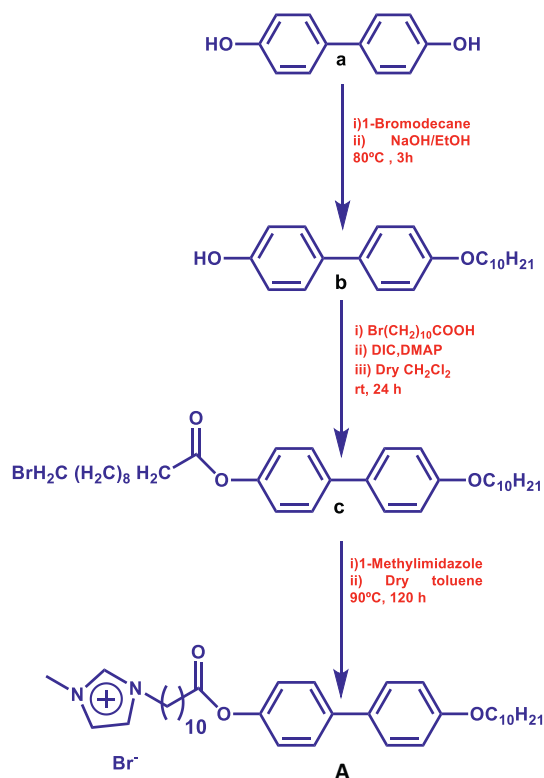
polished using a butter sheet, to get smooth and shiny appearance. The bare CPE was fabricated in the same manner without using ILC. ILC modified CPE fabricated at room temperature is referred as ILC-CPE-1. Two more ILC-CPE composite electrodes were prepared at two different temperatures of 90 °C and 120 °C (heating the ILC to the mentioned temperature and then mixing with graphite powder), which are called as ILC-CPE-2 and ILC-CPE-3 respectively.

3. Results and discussion

3.1. Synthesis and characterization of ILC

A new imidazolium based ILC compound bearing a biphenyl core was synthesized through a two-step approach of esterification followed by quaternisation as shown in Scheme 1. The synthesized compounds **b**, **c** and ILC, **A** were chemically characterized using a combination of FTIR, NMR and mass spectroscopic studies.

An FT-IR spectrum of ILC **A** along with the spectra for compounds **b** and **c** for comparison is provided in Fig. S1 (SI). IR spectrum of compound **b** showed a broad peak in the region 3400 to 3250 cm^{-1} corresponding to hydroxyl group. The peaks at 2933 cm^{-1} and 2855 cm^{-1} are due to C—H asymmetric and symmetric stretching vibrations. Compound **c** also showed IR bands corresponding to C—H stretching frequencies, however, additional bands were observed at 1735 cm^{-1} and at 1650 cm^{-1} due to C=O stretching (ester linkage) and C=C stretching of aromatic rings, which confirmed the successful esterification reaction. The FT-IR spectrum of ILC, **A** showed similar peaks at around same wavenumbers for ester linkage, C—H asymmetric, symmetric stretching and C=C stretching of aromatic rings. Additionally, a peak was observed at 1220 cm^{-1} due to C—N bending vibration which confirmed the presence of imidazolium moiety in the ILC. Moreover, the compounds **c** and **A** showed a broad band in the region 3500–3290 cm^{-1} , which is due to the moisture from the ambience.



Scheme 1. Synthesis of ILC compound **A**.

^1H NMR spectra of compound **c** along with peak assignment is given in Fig. S2 (SI). The characteristic peaks in the chemical shift range of 7.52–6.95 ppm correspond to aromatic protons of the biphenyl moiety (a, b, c, d). The triplet peak at 4.10 ppm is due to $-\text{OCH}_2$ protons attached to the biphenyl ring (e). The triplet peak at 3.42 ppm can be attributed to CH_2 protons attached to bromine atom (f) and triplet at 2.63 ppm can be ascribed to protons attached to the carbonyl group of the ester linkage (g). Furthermore, the multiplets observed in the chemical shift range of 2.01–1.35 ppm are due to rest of the 30 protons in the alkyl chains at both the ends of the biphenyl core. Additionally, triplet observed at 0.94 ppm can be attributed to the equivalent protons present in the terminal methyl group (j).

^1H and ^{13}C NMR spectra of ILC **A** along with peak assignment are provided in Figs. S3 and S4 (SI). ^1H spectrum of a ILC, **A** showed all the peaks observed in the spectrum of compound **c** almost at the same chemical shift values along with additional peaks at chemical shift values of 10.39, 7.35 and 4.12 ppm. A sharp singlet peak at 10.39 ppm is due to the proton present in between two nitrogen atoms in the imidazolium ring (k). The peak at chemical shift value of 7.35 corresponds to protons in the imidazolium moiety (m, n). Further, a sharp singlet observed at 4.12 ppm is due to the equivalent protons present in the methyl group (l) attached to the imidazolium ring. A high resolution mass spectrum of ILC, **A** is shown in Fig. S5 (SI). The measured molecular weight matched well with the calculated mass of 655.75.

3.2. Mesophase behaviour of ILC

Mesomorphic behaviour of the ILC **A** was investigated through differential scanning calorimetry (DSC), polarizing optical microscopy (POM) and X-ray diffraction (XRD) studies. Usually, on heating, LC compounds partially melt to lose their crystalline properties and show

mesophases with characteristic textural features which on further heating undergo a transition to an isotropic liquid state. A sample of ILC sandwiched between a normal glass slide and cover slip was heated to isotropic temperature and the textural observation was carried out on cooling from the isotropic melt. The mesophase developed from the isotropic as battonets at around 188 °C, which immediately turned to a homeotropic dark texture along with a little birefringence only around the edges of the air bubbles. These textural features correspond to a layered structure having an orthogonal arrangement of molecules with respect to the layer plane and hence indicate the presence of SmA phase having a uniaxial symmetry. On further cooling, at 143 °C, a low-birefringent schlieren texture developed over the pseudoisotropic region clearly indicating a phase transition. Interestingly, careful observation of the schlieren texture revealed the presence of both two-brush (strength $s = \pm 1/2$) and four-brush ($s = \pm 1$) disclinations. Further, similar textural observation was made for this mesophase, in a LC cell with the glass plates treated for homeotropic alignment instead of a dark/pseudoisotropic texture. The presence of both two- and four-brush defects rule out the occurrence of a tilted smectic C (SmC) phase, since only four-brush defects are exclusively observed for the SmC phase. These textural features speculate the presence of a biaxial SmA phase (SmA_b) [13] which was further investigated through conoscopy studies (described later). An additional change in the texture was observed at 93 °C and crystallisation was noticed at around 86 °C. The images of the sample showing a homeotropic texture of SmA phase at 158 °C, a schlieren texture at 134 °C and a fan-shaped texture at 88 °C, recorded on cooling from the isotropic phase, are shown in Fig. 1a, b and d respectively. An expanded version of a small area of the image 'b' is shown in Fig. 1c. Two more images showing a mixture of dark and bright regions in the SmA phase at 158 °C and a schlieren texture at 125 °C are provided in Fig. S6a and b (SI) respectively. The additional phase transition observed at 93 °C might correspond to a higher order

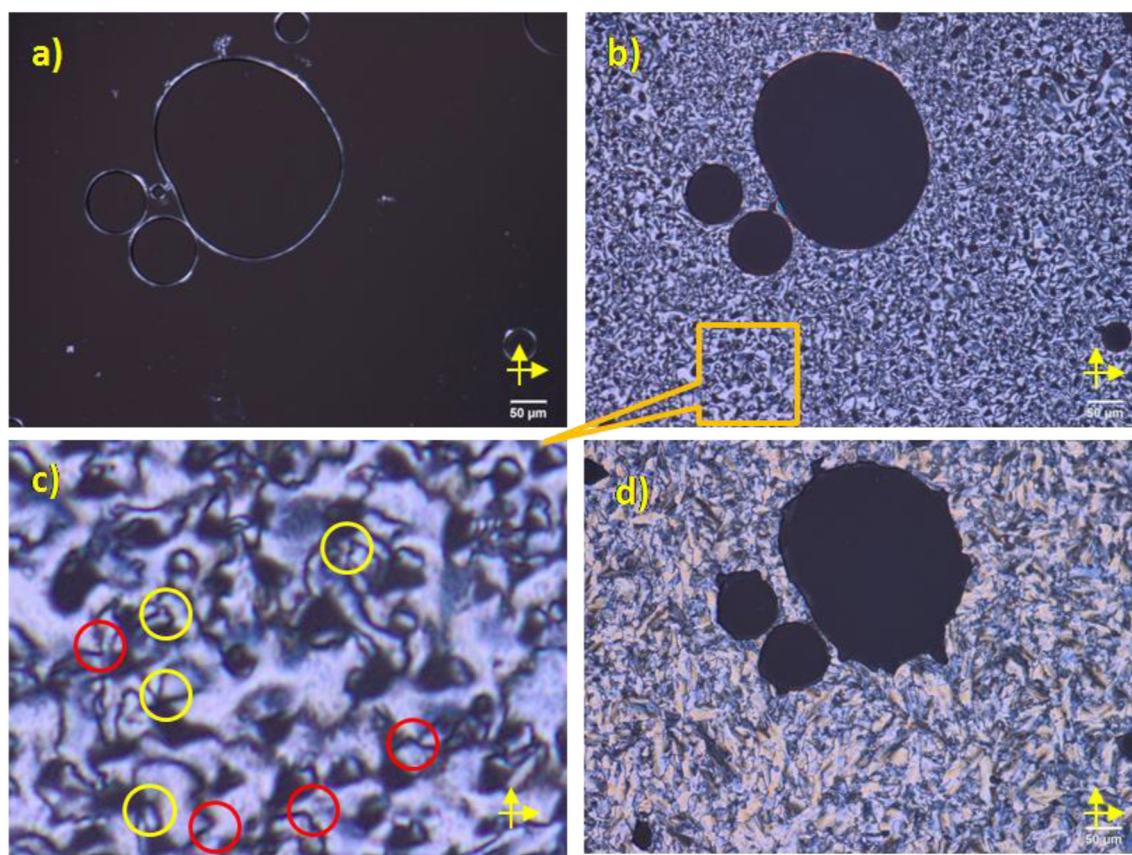


Fig. 1. POM images of ILC **A** held between a normal glass slide and a cover slip, at different temperatures recorded on cooling from the isotropic state; (a) at 158 °C (b) at 134 °C (c) a zoomed version of a small area of image 'b': yellow circles: four-brush defects, red circles: two-brush defects and (d) 88 °C.

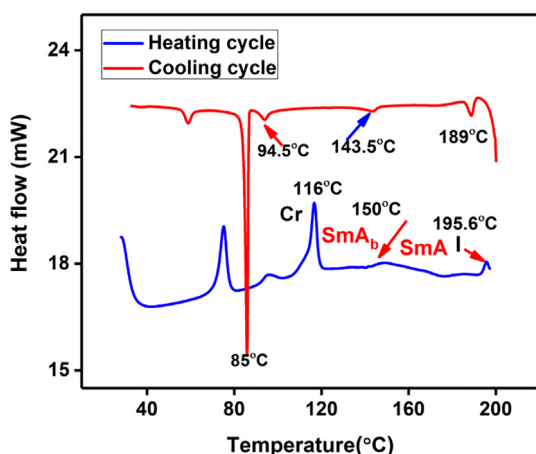


Fig. 2. DSC thermogram of ILC, A recorded at a heating and cooling rate of 10 °C/min.

smectic phase. However, XRD studies could not be carried out on this mesophase since the phase crystallised quickly. The thermal behaviour and phase transition temperatures were further confirmed through DSC studies.

A DSC thermogram of ILC recorded at a heating and cooling rate of 10 °C min⁻¹ is shown in Fig. 2. The sample showed a melting transition at 116 °C and another peak at 150 °C indicating a phase transition. The isotropic peak was observed at 195.6 °C. On cooling, the corresponding exothermic peaks were observed at 189 °C for isotropic to SmA phase and at 143.5 °C for the second transition. Another exothermic peak was observed at 94.5 °C, corresponding to a monotropic higher order smectic phase and crystallisation peak was recorded at 85 °C. Yet another small exothermic peak was observed at 60 °C which may correspond to a crystal-crystal transition. These transition temperature values matched well with those observed under POM. Although DSC showed two endothermic peaks on heating cycle, at 75.3 °C and 95.7 °C before the melting peak at 116 °C, these peaks were assigned to crystal-crystal transitions based on our POM observation. The sample melted at around 116.5 °C and the cover slip was able to be displaced only after this temperature. Based on these details and the conoscopy studies, we propose following phase behaviour for the ILC, A; Cr (SmX 94.5 °C) 116 °C SmA_b, 150 °C SmA 195.6 °C I.

3.3. Conoscopy experiment

Conoscopy experiment was carried out to confirm the uniaxial/biaxial nature of the low temperature SmA phase. For this experiment, well aligned sample in the form of free standing film was achieved as

follows; a loop was made at one end of a thin steel wire. The loop end of the wire was dipped into the sample taken in a sample cup and heated to the isotropic phase. As the wire is slowly pulled out there is a progressive decrease in temperature and the sample slowly transform into the smectic phase. During this process a uniform free standing film forms across the loop and stabilizes. The free standing film that is formed by this process not only has good stability but aligns well promoted by the drawing motion. A green filter was used and the crossed polarizers were at 45° and 135° in the POM for the observations. A typical uniaxial pattern was observed in the high temperature SmA phase at 185 °C. On lowering the temperature to 140 °C, the isogyres begin to split to give a biaxial pattern. However, the isogyres didn't split too much in the SmA_b phase. One possible reason is that the biaxial angle for this sample may be quite small. This confirms that the SmA_b phase exist at this temperature. Fig. 3 displays optical photomicrographs showing the patterns obtained in the uniaxial SmA (a) and biaxial SmA (b) phases of ILC A. Interestingly, when the alignment is not perfect we could observe the transition from SmA to SmA_b in the film under POM at temperatures where the difference in the conoscopic image can also be observed when alignment is good. These POM pictures are provided in Fig. 4a, b and c respectively.

3.4. XRD studies

XRD study of the ILC was performed as a function of temperature on cooling the sample from the isotropic melt. The X-ray angular intensity profiles at different temperatures are provided in Fig. 5a. The sample showed two reflections in the small angle region occurring at almost same 2θ values at all the measured temperatures. The *d* spacing was calculated to be $d_1 = 35.8 \text{ \AA}$ and $d_2 = 22.19 \text{ \AA}$ for the two peaks at 160 °C. The *d* spacing corresponding to the first reflection viz. $d_1 = 35.8 \text{ \AA}$ is smaller (by ~3.5 Å) than the measured molecular length ($L = 39.4 \text{ \AA}$, ACD/Chem sketch 3D viewer, Fig. S7, SI) considering an extended *all trans* conformation of the terminal alkyl chains, which suggests the possibility of the occurrence of a SmC phase. However, observation of the homeotropic texture for the sample placed in between a glass slide and cover slip (Fig. 1a) as well as in the free standing film (Fig. 4a) suggests an orthogonal arrangement of the molecules in layers, probably with an interdigitation of the alkyl chains in the adjacent layers. Interestingly the *d* spacing corresponding to the second reflection (d_2) is not exactly half of d_1 but is higher than $d_1/2$ by 4 Å. Further, intensity of the I and II peaks suggests the possibility of both d_1 and d_2 being repeating units [42]. Based on these details we propose an intercalated layer arrangement for the SmA phase, with a favourable overlapping of aromatic cores, alkyl chains and ionic moieties as shown in Fig. 5b. Such micro-segregation of ionic and non-ionic parts is known for the

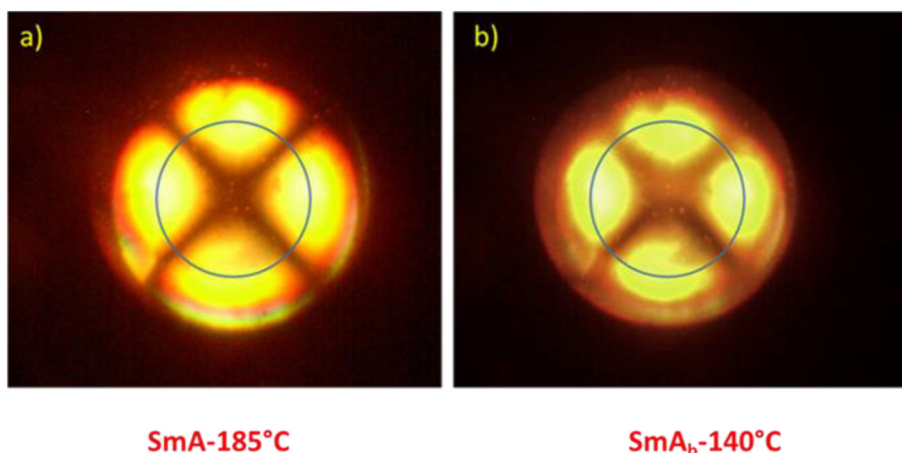


Fig. 3. Conoscopic images of ILC A (a) uniaxial SmA-185 °C (b) biaxial SmA_b-140 °C.

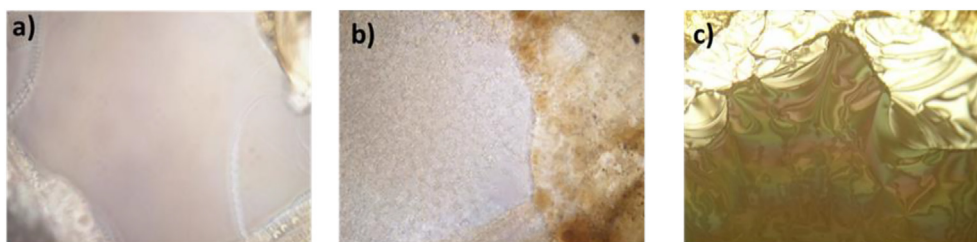


Fig. 4. POM images of ILC, A (a) uniaxial SmA-160 °C well aligned (b) SmA-SmA_B transition at 140 °C in well aligned sample (c) SmA-SmA_B transition at 140 °C, in sample which is not well aligned.

ILCs [43–45]. Additionally, the XRD patterns at both the temperatures exhibited a broad peak in the wide angle region at $2\theta = 18^\circ$ corresponding to a d spacing of 4.9 Å indicating a fluid like in-plane orientation. The XRD studies did not show any significant changes in the pattern or d values in the lower temperature phase (patterns at 140 °C, 130 °C, 120 °C and 100 °C). However, the POM observation and DSC studies clearly indicated the presence of two phases and conoscopic studies confirmed that these SmA phases are uniaxial and biaxial in nature at higher and lower temperature region respectively. Further, conoscopic experiments also revealed that the biaxial angle might be quite small for the lower temperature phase. This could be the reason for not observing any difference in the XRD pattern in these two phases. Nevertheless, occurrence of the two phases is confirmed through the textural changes observed for the sample in normal glass slides, free standing films and a corresponding transition peak in the DSC thermogram.

In addition to the textural observations using POM, ILC was also viewed under a scanning electron microscope (SEM). For the observation, sample was prepared by drop-casting a homogeneous solution of the ILC in chloroform on an ITO plate and dried under ambient conditions and directly examined under the microscope. Fascinatingly, hierarchical

array-like structures were observed on the surface due to self-assembling nature of the smectogenic ILC as shown in Fig. 6a and b. Additionally, SEM images of ILC-CP composite (prepared at different temperatures) are provided in Fig. S8 (SI).

3.5. Electrochemical characterization of ILC modified CPE electrodes

The electrochemical characteristics of the CPE and ILC modified CPEs were investigated using cyclic voltammetry technique (CV) in the potential range between -0.1 to 1 V at a scan rate of 50 mVs^{-1} in phosphate buffer solution (pH 7). The CVs obtained are provided in Fig. 7. The ILC modified electrodes showed two well defined oxidation peaks at the potential values of 0.2 and 0.6 V and their corresponding reverse peaks were also observed. Compared to CPE alone, the modified electrodes showed increased peak current suggesting good electron mediating property of the ILC. The cyclic voltammograms of ILC modified electrodes fabricated at room temperature (ILC-CPE-1), 90 °C (ILC-CPE-2) and 120 °C (ILC-CPE-3) exhibited almost same electrochemical response with a slight potential shifts in the positive direction. For ILC-CPE-3 fabricated at 120 °C, the anodic peak current was 0.086 mA at

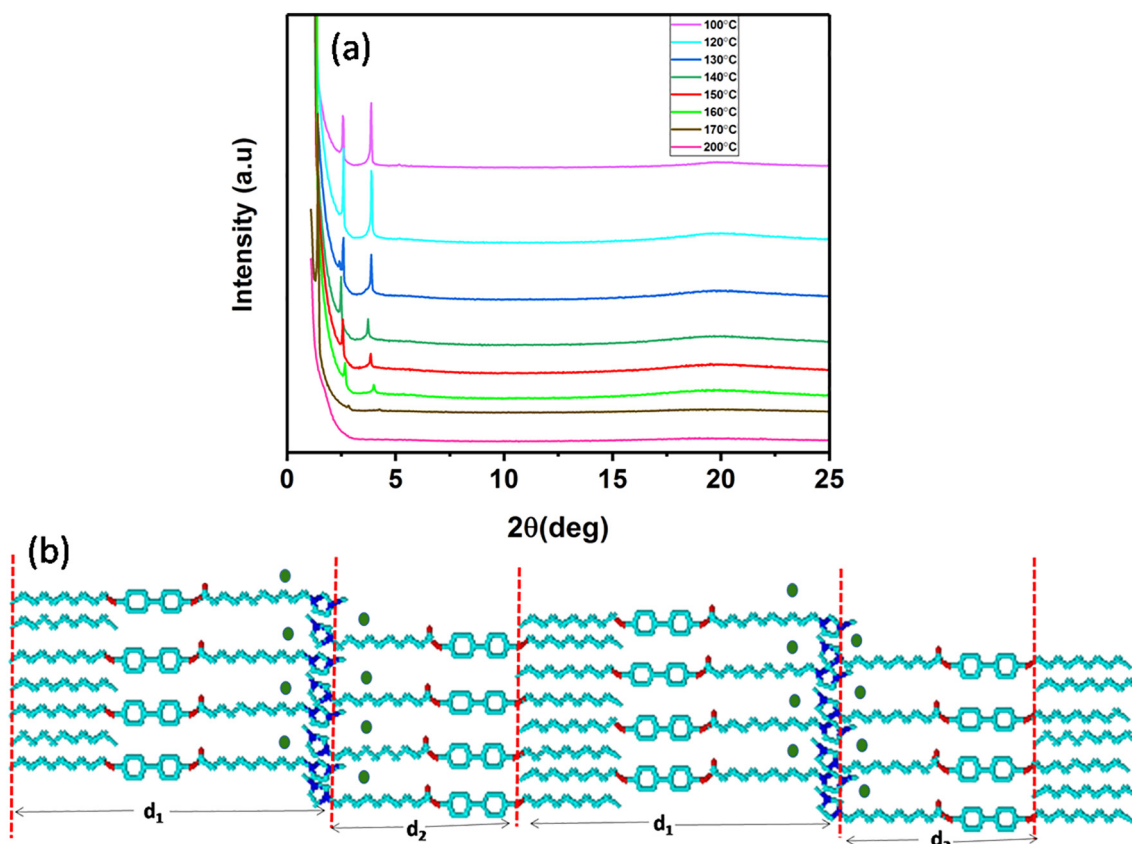


Fig. 5. (a) XRD pattern of ILC, A as a function of temperature recorded on cooling from the isotropic phase and (b) a schematic representation of the molecular arrangement in the mesophase.

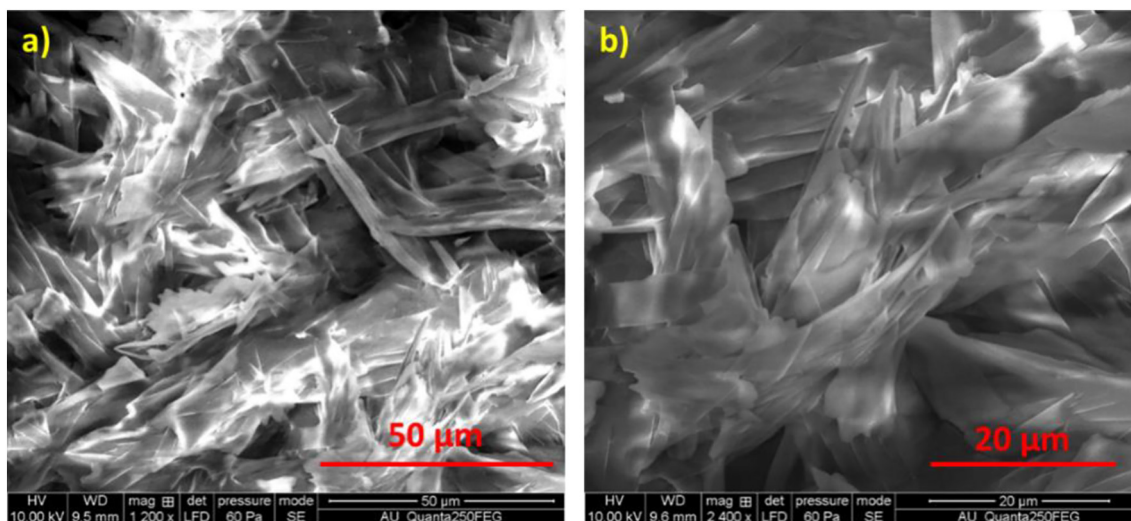


Fig. 6. (a) & (b) Representative SEM images of the ILC, A at different magnification.

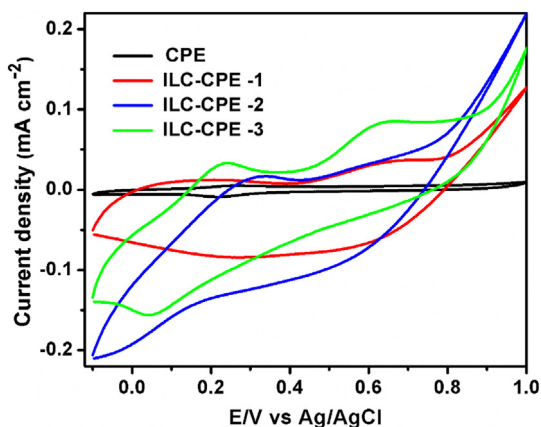


Fig. 7. Cyclic voltammograms of CPE and ILC-CPE-1, ILC-CPE-2 and ILC-CPE-3 recorded in phosphate buffer solution at a scan rate of 50 mVs^{-1} .

0.63 V which is higher than that obtained at other electrodes indicating the rapid electron transfer property. Therefore, ILC-CPE-3 fabricated at 120°C was considered as optimized electrode and further experiments were carried out using the same.

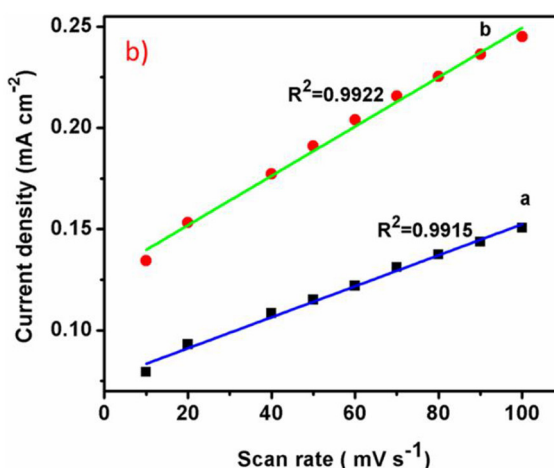
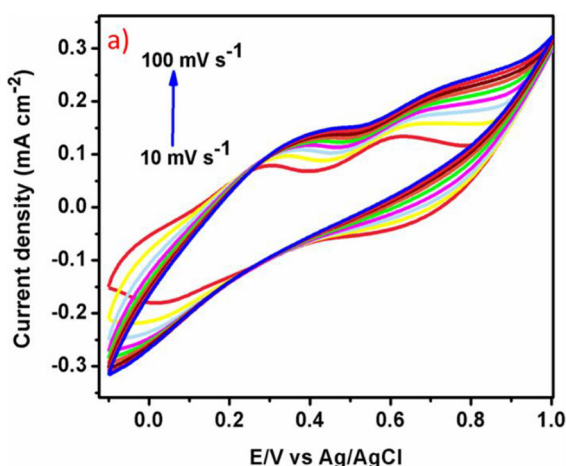


Fig. 8. (a) Cyclic voltammetry response of ILC-CPE-3 at different scan rates ($10\text{--}100 \text{ mVs}^{-1}$); (b) linear plot of anodic (a) and cathodic (b) peak current vs scan rates.

3.6. Effect of scan rate

In order to study the electrode kinetics of ILC-CPE-3, CVs at different scan rate were recorded from 10 to 100 mVs^{-1} which are shown in Fig. 8a. On increasing the scan rate, anodic and cathodic peak current was gradually increased with minor potential shifts in the anodic direction which is a typical behaviour of a reversible system. The resultant anodic and cathodic peak current was plotted against the scan rate that yielded a linear behaviour with correlation coefficient of 0.9915 and 0.9922 respectively, and the linear dependence plot is shown in Fig. 8b. These results revealed that the electrochemical reaction is entirely a surface confined process which is in good agreement with the literature report [46,47].

3.7. Electrocatalytic oxidation of paracetamol

The electrocatalytic activity of CPE and ILC-CPE-3 towards oxidation of paracetamol was ascertained from their CV response recorded in phosphate buffer solution (pH 7) at a scan rate of 50 mVs^{-1} . The electro-oxidation of paracetamol at the modified electrode is shown in Fig. 9a. For every addition of paracetamol into the electrochemical cell, the modified electrode responded rapidly with increment in the anodic

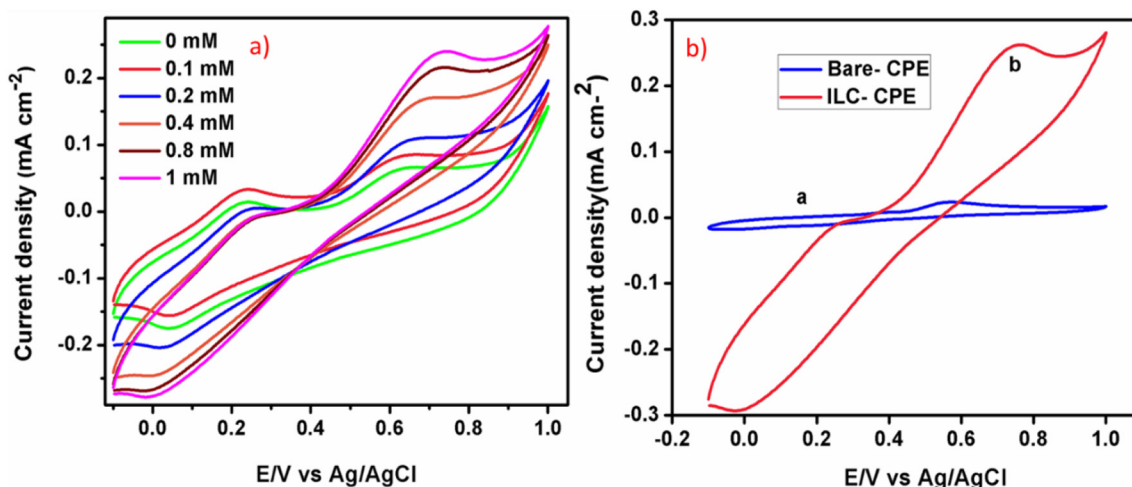


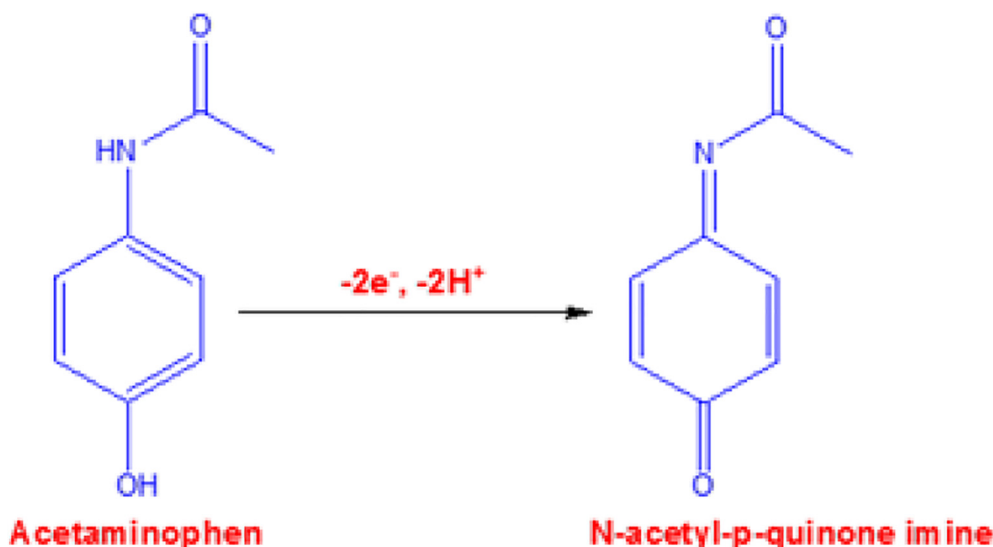
Fig. 9. (a) CV curves of ILC-CPE-3 in presence of various concentrations of paracetamol in phosphate buffer solution at a scan rate of 50 mVs^{-1} (b) comparison CVs of CPE and ILC-CPE in presence of 1 mM paracetamol.

peak current. On increasing the concentration of paracetamol from 0.1 mM to 1 mM, the anodic peak at 0.63 V was enhanced with simultaneous decrease in the reduction current and the potential was also shifted towards the negative direction, which implies that the presented sensor reduces the overpotential. These results inferred the good electrocatalytic activity of the proposed electrode material. The electrocatalytic activity could be due to self-assembled and highly ordered nature of the ILC containing CPE electrode material. This layered morphology can induce more edge-plane-like defects on the surface which in turn can increase the kinetics of the electrode reaction [27]. Porous surface of CP coupled with ordered nature of ILC, facilitates good ionic mobility and drug molecule penetration. Fig. 9b shows the cyclic voltammograms of CPE and ILC-CPE-3 in presence of 1 mM of paracetamol recorded at a scan rate of 50 mVs^{-1} . When 1 mM of paracetamol was added, the unmodified CP electrode exhibited an anodic oxidation peak with I_{pa} of 0.024 mA at 0.6 V. But, the ILC modified electrode (ILC-CPE-3) displayed an enhanced oxidation peak having $I_{pa} = 0.262 \text{ mA}$ at 0.75 V. About 10 fold increase in oxidation peak current was observed for ILC-CPE-3, compared to CPE alone. Though the unmodified CP electrode has less overpotential, the onset potential of paracetamol oxidation starts earlier at modified electrode, which revealed the excellent electrocatalytic activity of ILC-CPE-3. The electro-

oxidation mechanism of paracetamol is shown in Scheme 2. These results clearly suggest that the incorporation of ILC in CP could make them suitable candidate for the fabrication of electrochemical sensor for real time applications.

3.8. Differential pulse voltammetric studies

Differential pulse voltammetry (DPV) with a frequency of 10 Hz and amplitude of 10 mV potential possess higher sensitivity and better resolution than CV. Hence, the electrochemical determination of paracetamol using ILC-CPE-3 was studied using DPV technique in the potential range from 0.4 V to 0.8 V. Fig. 10a presents the DPV curves for increasing concentrations of paracetamol from $0 \mu\text{M}$ to $200 \mu\text{M}$. Upon every addition of paracetamol, the oxidation peak current increased and the peak potential also shifted towards more negative potential suggesting the electro oxidizing capability of paracetamol. In order to extract the analytical parameters such as limit of detection, sensitivity and linear range, the calibration curve was plotted against various paracetamol concentrations with their corresponding oxidation peak currents and the plot is shown in Fig. 10b. A linear relationship was achieved from $0 \mu\text{M}$ to $120 \mu\text{M}$ with the correlation coefficient of 0.9995. The slope value of the linear calibration curve gives the sensitivity and it was



Scheme 2. Electrochemical oxidation of acetaminophen(paracetamol) to N-acetyl-p-quinone imine

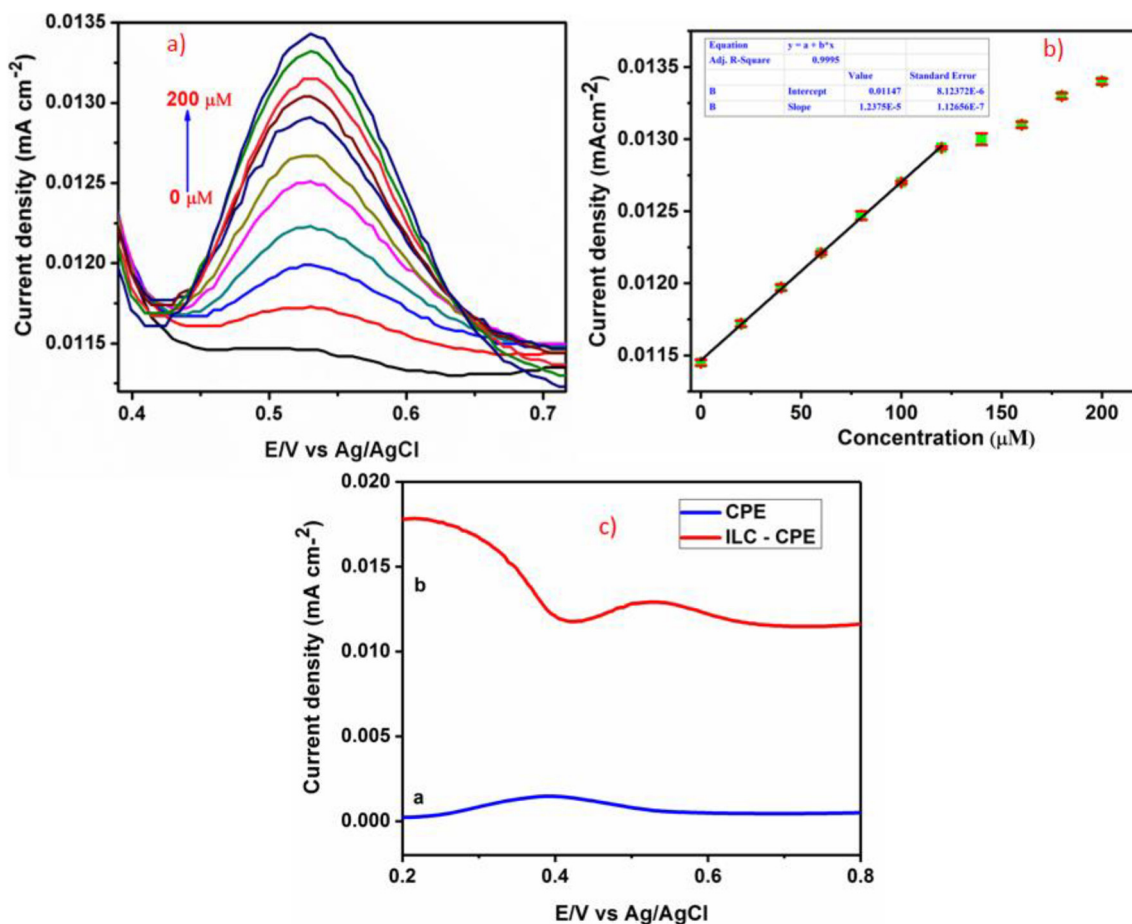


Fig. 10. (a) DPV response of ILC-CPE-3 for increasing concentration of paracetamol (b) the corresponding linear calibration plot between concentration and current (c) comparison DPV curves for CPE and ILC-CPE-3 in presence of paracetamol.

calculated as $0.0123 \mu\text{A } \mu\text{M}^{-1} \text{ cm}^{-2}$. The detection limit was calculated using the following equation

$$\text{LOD} = 3 s/m$$

where, 3 is the signal to noise ratio and 's' is the standard deviation and 'm' is the slope of the linear calibration curve. The detection limit was estimated as $2.8 \mu\text{M}$, which is a good detection limit for the pure ILC-graphite based composite electrodes without any metal/metal oxide doping. Table 1 summarizes the analytical performance of different types of modified electrodes for paracetamol detection, reported in the literature. It was found that the developed ILC modified CPE sensor showed acceptable limit of detection and sensitivity. The ILC modified CPE showed excellent oxidation current response for paracetamol than that of unmodified CPE. The comparison DPV curves are presented in Fig. 10c.

3.9. Interference studies

Selectivity is an important factor associated with electrochemical sensor fabrication because there are some intermediates interfere with paracetamol in pharmaceutical synthesis. Fig. 11a depicts the influence of the interfering compounds towards electro-oxidation of paracetamol. DPV curves were recorded by addition of 10 fold increased concentration of glucose, ascorbic acid, uric acid, dopamine, and 5 fold increased concentration of KCl, CuSO_4 and nitrophenol along with $50 \mu\text{M}$ of paracetamol. The DPV current response for addition of interferents was only 3% [50] which is insignificant compared to that of paracetamol and is depicted in Fig. 11b. The ILC-CPE modified electrode detected paracetamol even in the presence of mixture of interferents that suggested the anti-interfering ability. Hence, the present sensor material could be used for the assay of paracetamol in practical applications.

Table 1

Comparison of different modified electrodes reported for electrochemical sensing of paracetamol.

Modified electrodes	Linear range (μM)	Detection limit (μM)	Sensitivity $\mu\text{A } \mu\text{M}^{-1} \text{ cm}^{-2}$	References
C60/GCE	50–1500	50	13.04	[47]
Dipyrrromethene-Cu(II)/Au	–	120	–	[48]
β -CD/RGO/GCE	10–800	2.3	–	[49]
Co-Ni/copper foam	10–100	2.7	7960	[34]
ILC-CPE	0–120	2.8	0.0123	Present work

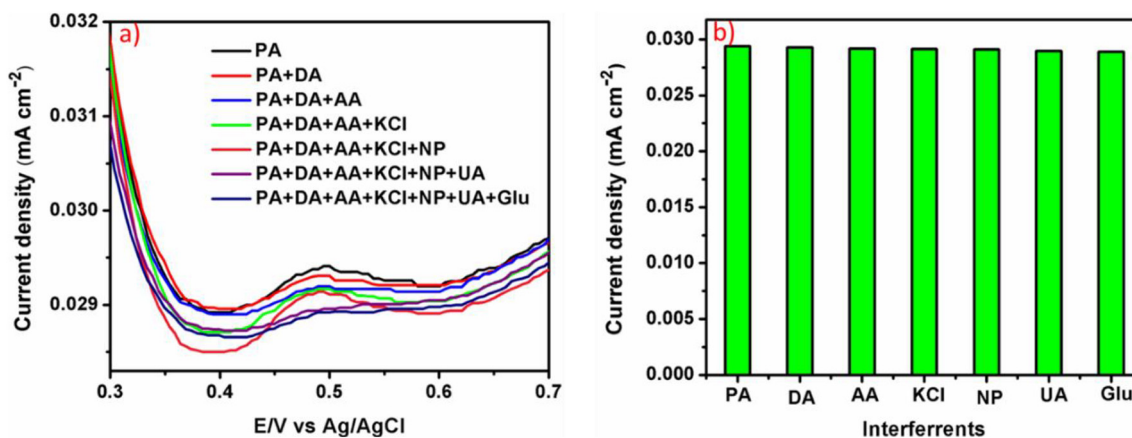


Fig. 11. (a) DPV curves of ILC-CPE-3 modified electrode in presence of 50 μM of paracetamol and 5 fold increased concentration of other possible interferents (b) corresponding bar graph for the data shown in Fig. 11a.

3.10. Reproducibility and stability test

The reproducibility of the ILC modified CPE electrode was evaluated using DPV technique. For that, five different ILC modified electrodes were fabricated under same experimental conditions and the DPV curves were recorded. Interestingly, upon addition of 50 μM of paracetamol, all the five modified electrodes gave similar oxidation peak current response. Based on the current response of five modified electrodes, the relative standard deviation was calculated as 3.5% which suggested the excellent reproducibility of the proposed electrode. The electrode to electrode reproducibility was also tested by adding 50 μM of paracetamol with time intervals of every 4 h. Whenever, the paracetamol was added, the ILC modified CPE electrode gave similar oxidation peak current with slight fluctuations. The modified electrode stability was also investigated for every five days over a period of one month. About 92.6% of oxidation peak current was retained after 1 month revealing the good stability of ILC modified CPE electrode.

3.11. Real sample studies

The practicability of ILC-CPE-3 electrode towards paracetamol was evaluated from DPV current response using standard addition method. For that, paracetamol (500 mg) tablet was finely ground in the mortar and accurately weighed and the stock solution was prepared. Pond water was collected from nearby location and diluted with phosphate buffer solution without further treatment. Usually, dilution is done to reduce the matrix effect of the real samples. As expected, addition of pond water in PBS, the proposed electrode did not show any electrochemical response but, for addition of 10 μM of paracetamol into the same solution exhibited an oxidation peak at approximately 0.58 V confirming the oxidation of paracetamol. Further, addition of increased concentration of the sample (20 and 30 μM), the oxidation peak current enhanced suggesting the practical utilization in real samples. The spiked concentrations coincided well with the concentration in the calibration curve. The recovery results were obtained and listed in Table 2 which are in the range of 99 to 102% revealing the good feasibility of our proposed electrode material.

Table 2
Determination of paracetamol in pharmaceutical samples.

Sample	Added (μM)	Found (μM)	Recovery (%)	RSD (%)
Paracetamol (500 mg tablet)	10	10.2	102	1.6
	20	19.8	99	2.3
	30	30.3	101	1.2

RSD-relative standard deviation.

4. Conclusions

In summary, a new ILC containing biphenyl core bearing a terminal imidazolium moiety was synthesized which exhibited two enantiotropic smectic A (SmA) phases having a biaxial and uniaxial nature. Electrochemical studies of the ILC as an electrode material in combination with carbon paste showed increased current response compared to carbon paste alone, suggesting a good electron mediating property of the ILC. The ILC-CPE electrode was analysed for the electrochemical detection of an analgesic drug paracetamol. The proposed sensor material exhibited excellent electrocatalytic activity, reproducibility, stability and anti-interfering ability. The differential pulse voltammetry experiments yielded a linear range from 0 to 120 μM with good detection limit of 2.8 μM for the sensing of paracetamol. Direct determination of the paracetamol in pharmaceutical formulation was successfully conducted using the ILC-CP electrode.

CRedit authorship contribution statement

R. Mangaiyarkarasi: Methodology, Investigation, Validation, Writing - original draft. **S. Premlatha:** Investigation, Writing - original draft. **Rajkumar Khan:** Investigation. **R. Pratibha:** Investigation, Writing - review & editing, Supervision. **S. Umadevi:** Conceptualization, Writing - review & editing, Supervision, Project administration, Funding acquisition.

Declaration of competing interest

The authors declare that they have no known competing financial interests or personal relationships that could have appeared to influence the work reported in this paper.

Acknowledgements

The authors would like to acknowledge the financial support from RUSA-Phase 2.0 grant, MHRD sanctioned vide Letter No. F. 24-51/2014-U, Dt.09.10.2018 and DST PURSE-II, New Delhi. Authors would like to thank USIC, Alagappa University for SEM analysis and National Institute of Technology, Tiruchirapalli for DSC analysis. Authors thank Mrs. K. N. Vasudha, Raman Research Institute, Bengaluru for help in XRD measurements.

Appendix A. Supplementary data

Spectroscopic data for the synthesized compounds, ACD chemlab 3D viewer of ILC A, POM and SEM images. Supplementary data to this

article can be found online at <https://doi.org/10.1016/j.molliq.2020.114255>.

References

- [1] T. Kato, J. Uchida, T. Ichikawa, T. Sakamoto, Functional liquid crystals towards the next generation of materials, *Angew. Chem. Int. Ed.* 57 (2018) 4355–4371.
- [2] S. Umadevi, B.K. Sadashiva, Novel five-ring bent-core compounds exhibiting a transition from the electro-optically non-switchable to a switchable B₇ phase, *Chem. Mater.* 18 (2006) 5186–5192.
- [3] S. Umadevi, S. Radhika, B.K. Sadashiva, The SmCP_A phase in five-ring bent-core compounds derived from 5-methoxyisophthalic acid, *Liq. Cryst.* 33 (2006) 139–147.
- [4] S. Umadevi, R. Umamaheswari, V. Ganesh, Lyotropic liquid crystal-assisted synthesis of micro- and nanoparticles of silver, *Liq. Cryst.* 44 (2017) 1409–1420.
- [5] B. Sivaranjini, R. Mangaiyarkarasi, V. Ganesh, S. Umadevi, Vertical alignment of liquid crystals over a functionalized flexible substrate, *Sci. Rep.* 8 (2018) 8891.
- [6] K. Binnemans, Ionic liquid crystals, *Chem. Rev.* 105 (2005) 4148–4204.
- [7] K. Goossens, K. Lava, C.W. Bielawski, K. Binnemans, Ionic liquid crystals: versatile materials, *Chem. Rev.* 116 (2016) 4643–4807.
- [8] R. Mangaiyarkarasi, B. Sivaranjini, S. Umadevi, Facile synthesis of gold nanoparticles capped with an ammonium-based chiral ionic liquid crystal, *Liq. Cryst.* 46 (2019) 584–593.
- [9] P.G. de Gennes, J. Prost, The physics of liquid crystals, *International Series of Monographs on Physics* 83 (1993) 597.
- [10] H. Friedrich, L. Heino, Optical investigations on a liquid-crystalline side-chain polymer with biaxial nematic and biaxial smectic A phase, *Makromol. Chem.* 192 (1991) 1317–1328.
- [11] R. Pratibha, N.V. Madhusudana, B.K. Sadashiva, An orientational transition of bent-core molecules in an anisotropic matrix, *Science* 288 (2000) 2184–2187.
- [12] T. Hegmann, J. Kain, S. Diele, G. Pelzl, C. Tschierske, Evidence for the existence of the McMillan phase in a binary system of a metallomesogen, *Angew. Chem. Int. Ed.* 40 (2001) 887–890.
- [13] C.V. Yelamagadda, I.S. Shashikala, D.S.S. Rao, G.G. Nair, S.K. Prasad, The biaxial smectic (SmA_b) phase in nonsymmetric liquid crystal dimers comprising two rod like anisometric segments: an unusual behavior, *J. Mater. Chem.* 16 (2006) 4099–4102.
- [14] M. Yoshio, T. Mukai, H. Ohno, T. Kato, One-dimensional ion transport in self-organized columnar ionic liquids, *J. Am. Chem. Soc.* 126 (2004) 994–995.
- [15] J. Sakuda, M. Yoshio, T. Ichikawa, H. Ohno, T. Kato, 2D assemblies of ionic liquid crystals based on imidazolium moieties: formation of ion-conductive layers, *New J. Chem.* 39 (2015) 4471–4477.
- [16] R. Sasi, S. Sarojam, S.J. Devaki, High performing bio ionic liquid crystal electrolytes for supercapacitors, *ACS Sustain. Chem. Eng.* 4 (2016) 3535–3543.
- [17] F. Yuan, S. Chi, S. Dong, X. Zou, S. Lv, L. Bao, J. Wang, Ionic liquid crystal with fast ion-conductive tunnels for potential application in solvent-free Li-ion batteries, *Electrochim. Acta* 294 (2019) 249–259.
- [18] N.F. Atta, A. Galal, S.M. Azab, A.H. Ibrahim, Electrochemical sensor based on ionic liquid crystal modified carbon paste electrode in presence of surface active agents for enoxacin antibacterial drug, *J. Electrochem. Soc.* 162 (2014) 9–15.
- [19] R. Mangaiyarkarasi, S. Selvam, V. Ganesh, S. Umadevi, A cholesterol based imidazolium ionic liquid crystal: synthesis, characterisation and its dual application as an electrolyte and electrode material, *New J. Chem.* 43 (2019) 1063–1071.
- [20] I. Švancara, K. Vytras, J. Barek, J. Zima, Carbon paste electrodes in modern electroanalysis, *Crit. Rev. Anal. Chem.* 31 (2001) 311–345.
- [21] S.S. Shankar, R.M. Shereema, R.B. Rakhi, Electrochemical determination of adrenaline using MXene/graphite composite paste electrodes, *ACS. Appl. Mater. Interface* 50 (2018) 43343–43351.
- [22] M.D.P.T. Sotomayor, A. La Rosa-toro, Development of a new electrochemical sensor based on silver sulfide nanoparticles and hierarchical porous carbon modified carbon paste electrode for determination of cyanide in river water samples, *Sens. Actuators B: Chem.* 287 (2019) 544–550.
- [23] N. Maleki, A. Safavi, F. Tajabadi, High-performance carbon composite electrode based on an ionic liquid as a binder, *Anal. Chem.* 78 (2006) 3820–3826.
- [24] H. Beitollahi, S. Ghofrani, M. Torkezadeh-mahani, Application of antibody – nanogold – ionic liquid – carbon paste electrode for sensitive electrochemical immunoassay of thyroid-stimulating hormone, *Biosens. Bioelectron.* 110 (2018) 97–102.
- [25] A. Alvarez Fernandez, P.H.J. Kouwer, Key developments in ionic liquid crystals, *Int. J. Mol. Sci.* 17 (2016) 731–736.
- [26] C.E. Banks, T.J. Davies, G.G. Wildgoose, R.G. Compton, Electrocatalysis at graphite and carbon nanotube modified electrodes: edge-plane sites and tube ends are the reactive sites, *Chem. Commun.* (2005) 829–841.
- [27] A. Safavi, M. Tohidi, Design and characterization of liquid crystal - graphite composite electrodes, *J. Phys. Chem.* 114 (2010) 6132–6140.
- [28] N.F. Atta, A.H. Ibrahim, A. Galal, Nickel oxide nanoparticles/ionic liquid crystal modified carbon composite electrode for determination of neurotransmitters and paracetamol, *New J. Chem.* 40 (2016) 662–673.
- [29] N.F. Atta, S.A. Abdel Gawad, E.H. El-Ads, A.R.M. El-Gohary, A. Galal, A new strategy for NADH sensing using ionic liquid crystals-carbon nanotubes/nano-magnetite composite platform, *Sens. Actuators B: Chem.* 251 (2017) 65–73.
- [30] J.A.H. Forrest, J.A. Clements, L.F. Prescott, Clinical pharmacokinetics of paracetamol, *Clin. Pharmacokinet.* 7 (1982) 93–107.
- [31] M.T. Olaleye, B.T. Joa, Acetaminophen-induced liver damage in mice: effects of some medicinal plants on the oxidative defense system, *Exp. Toxicol. Pathol.* 59 (2008) 319–327.
- [32] R. Beasley, T. Clayton, J. Crane, E. Von Mutius, C.K.W. Lai, S. Montefort, A. Stewart, Association between paracetamol use in infancy and childhood, and risk of asthma, rhinoconjunctivitis, and eczema in children aged 6 – 7 years: analysis from phase three of the ISAAC programme, *Lancet* 372 (2008) 1039–1048.
- [33] S. Gupta, S. Chatterjee, A.K. Ray, A.K. Chakraborty, Chemical graphene – metal oxide nanohybrids for toxic gas sensor: a review, *Sens. Actuators B: Chem.* 221 (2015) 1170–1181.
- [34] S. Premalatha, G.N.K.R. Babu, Fabrication of Co-Ni alloy nanostructures on copper foam for highly sensitive amperometric sensing of acetaminophen, *J. Electroanal. Chem.* 822 (2018) 33–42.
- [35] B. Adhikari, M. Govindhan, A. Chen, Sensitive detection of acetaminophen with graphene-based electrochemical sensor, *Electrochim. Acta* 162 (2015) 198–204.
- [36] E. Bayram, E. Akyilmaz, Development of a new microbial biosensor based on conductive polymer/multiwalled carbon nanotube and its application to paracetamol determination, *Sens. Actuators B: Chem.* 233 (2016) 409–418.
- [37] R.H.G. Mingels, S. Kalsi, Y. Cheong, H. Morgan, Iridium and ruthenium oxide miniature pH sensors: long-term performance, *Sens. Actuators B: Chem.* 297 (2019), 126779.
- [38] A. Galal, N.F. Atta, S.M. Azab, A.H. Ibrahim, Electroanalysis of benazepril hydrochloride antihypertensive drug using an ionic liquid crystal modified carbon paste electrode, *Electroanalysis* 27 (2015) 1282–1292.
- [39] N.F. Atta, M. BinSabt, S. Hassan, A. Galal, Ionic liquid crystals modifier for selective determination of terazosin antihypertensive drug in presence of common interference compounds, *Crystals* 7 (2017) 27.
- [40] N.F. Atta, E.H. El-ads, S.H. Hassan, A. Galal, Surface modification of carbon paste electrode with nano-structured modifiers: application for sub-nano-sensing of paracetamol, *J. Electrochem.* 164 (2017) 519–527.
- [41] N.F. Atta, A. Galal, E.H. El-ads, M. Ahmed, Determination of some neurotransmitters at cyclodextrin/ionic liquid crystal/graphene composite electrode, *Electrochim. Acta* 199 (2016) 319–331.
- [42] K. Kishikawa, T. Inoue, N. Hasegawa, M. Takahashi, M. Kohri, T. Taniguchi, S. Kohmoto, Achiral straight-rod liquid crystals indicating local biaxiality and ferroelectric switching behavior in the smectic A and nematic phases, *J. Mater. Chem. C* 3 (2015) 3574–3581.
- [43] K. Goossens, P. Nockemann, K. Driesen, B. Goderis, C. Görlner-walrand, K. Van Hecke, L. Van Meervelt, E. Pouzet, K. Binnemans, T. Cardinaels, Imidazolium ionic liquid crystals with pendant mesogenic groups, *Chem. Mater.* 20 (2008) 157–168.
- [44] X. Lan, L. Bai, X. Li, S. Ma, X. He, F. Meng, Cholesteryl-containing ionic liquid crystals composed of alkylimidazolium cations and different anions, *J. Mol. Struct.* 1075 (2014) 515–524.
- [45] B.T. Heng, G. Yeap, W. Ahmad, K. Mahmood, C. Han, H.C. Lin, S. Takanoc, D. Takeuchi, Alkyl chain self ordering, induction and suppression of mesophase by Cu (II) containing [1,2,3]-triazole-based bidentate salicylaldehyde ligands: synthesis, characterisation and X-ray diffraction studies, *Liq. Cryst.* 41 (2014) 37–41.
- [46] Y.E.L. Bouabi, A. Farahi, N. Labjar, S. El Hajjaji, M. Bakasse, M.A. El Mhammedi, Square wave voltammetric determination of paracetamol at chitosan modified carbon paste electrode: application in natural water samples, commercial tablets and human urines, *Mater. Sci. Eng. C* 58 (2016) 70–77.
- [47] R.N. Goyal, S.P. Singh, Voltammetric determination of paracetamol at C60-modified glassy carbon electrode, *Electrochim. Acta* 51 (2006) 3008–3012.
- [48] B. Saraswathyamma, I. Grzybowska, C. Orlewska, J. Radecki, W. Dehaen, K.G. Kumar, H. Radecka, Electroactive dipyrromethene-Cu (II) monolayers deposited onto gold electrodes for voltammetric determination of paracetamol, *Electroanalysis* 20 (2008) 2317–2323.
- [49] G. Lai, A. Yu, Preparation of β-cyclodextrin functionalized reduced graphene oxide: application for electrochemical determination of paracetamol, *RSC Adv.* 5 (2015) 76973–76978.
- [50] N. Karikalan, R. Karthik, S.M. Chen, H.A. Chen, A voltammetric determination of caffeic acid in red wines based on the nitrogen doped carbon modified glassy carbon electrode, *Sci. Rep.* 7 (2017), 45924.